

Enhanced damage accumulation in carbon implanted silicon

J. P. de Souza, H. Boudinov, and P. F. P. Fichtner

Citation: [Applied Physics Letters](#) **64**, 3596 (1994); doi: 10.1063/1.111209

View online: <http://dx.doi.org/10.1063/1.111209>

View Table of Contents: <http://scitation.aip.org/content/aip/journal/apl/64/26?ver=pdfcov>

Published by the [AIP Publishing](#)

Articles you may be interested in

[Comprehensive model of damage accumulation in silicon](#)

J. Appl. Phys. **103**, 014911 (2008); 10.1063/1.2829815

[Damage accumulation in neon implanted silicon](#)

J. Appl. Phys. **100**, 043505 (2006); 10.1063/1.2220644

[Structural characterization and modeling of damage accumulation in In implanted Si](#)

J. Appl. Phys. **95**, 150 (2004); 10.1063/1.1631076

[Strain development and damage accumulation during neon ion implantation into silicon at elevated temperatures](#)

J. Appl. Phys. **88**, 1771 (2000); 10.1063/1.1305928

[Boron channeling implantations in silicon: Modeling of electronic stopping and damage accumulation](#)

J. Appl. Phys. **77**, 3697 (1995); 10.1063/1.358608

A promotional banner for Applied Physics Reviews. On the left is a thumbnail of a journal cover for 'Applied Physics Reviews' featuring a diagram of a layered structure. The main text reads 'NEW Special Topic Sections' in large white letters on a blue background. Below this, it says 'NOW ONLINE' in yellow, followed by 'Lithium Niobate Properties and Applications: Reviews of Emerging Trends' in white. The AIP logo and 'Applied Physics Reviews' are in the bottom right corner.

NEW Special Topic Sections

NOW ONLINE
Lithium Niobate Properties and Applications:
Reviews of Emerging Trends

AIP Applied Physics
Reviews

Enhanced damage accumulation in carbon implanted silicon

J. P. de Souza and H. Boudinov
Instituto de Física, UFRGS, 91501-970 Porto Alegre, R.S., Brazil

P. F. Fichtner
Escola de Engenharia, UFRGS, 90035-190 Porto Alegre, R.S., Brazil

(Received 20 December 1993; accepted for publication 12 April 1994)

The accumulation of damage in Si implanted with $^{12}\text{C}^+$ was investigated experimentally using aligned Rutherford backscattering analysis. The damage profiles in Si implanted with $^{12}\text{C}^+$ or $^{11}\text{B}^+$ at 50 keV to the same doses and dose rate were compared. It was found that the damage accumulates at a noticeably higher rate by $^{12}\text{C}^+$ implantation than by $^{11}\text{B}^+$, especially for doses $>2 \times 10^{15} \text{ cm}^{-2}$. In order to explain our results we suggest that self-interstitial Si atoms are captured by the implanted C atoms, forming complex defects which are stable at room temperature.

The ion implantation is presently a routine doping process in silicon integrated circuit technology. It is well known that ion implantation introduces radiation damage, which may be detrimental to the electronic device performance. Partial annealing of the damage occurs concomitantly with the implantation process and this phenomenon is called dynamic annealing. The dynamic annealing is known to be more pronounced for light mass ion implantation, low dose rate, and heated substrates. The extent of this *in situ* annealing determines the final as-implanted damage concentration and consequently strongly influences the choice of the post-implantation annealing regime, required for efficient damage repairing.

In the present investigation, the as-implant damage concentration in $^{12}\text{C}^+$ implanted Si is compared with that by $^{11}\text{B}^+$. Since the masses of these ions are nearly equal, almost similar collision cascade properties and primary defect production rates are expected to occur when their energy and dose rate are identical. However, in contrast to this prediction, the actual damage profiles due to $^{11}\text{B}^+$ and $^{12}\text{C}^+$ implants at an energy of 50 keV, performed to the same doses, differ significantly particularly for doses in excess to $1 \times 10^{15} \text{ cm}^{-2}$. For example, the damage concentration level after $^{12}\text{C}^+$ implantation to a dose $4 \times 10^{15} \text{ cm}^{-2}$ results about ten times higher than that of $^{11}\text{B}^+$. This seems to indicate that the dynamic annealing is strongly influenced by the chemical nature of carbon.

Besides oxygen, carbon is the most widely discussed impurity in Si and it is known to affect many different phenomena in the crystal.¹⁻⁵ Recent investigations demonstrated that by C^+ implantation it is possible to reduce the transient enhanced diffusion⁶ and prevent dislocation formation in Si coimplanted with B^+ .⁷ In addition, the electrical activation of implanted B is significantly influenced by a C^+ coimplantation such that the reverse annealing phenomenon can be suppressed.⁸ All these mentioned facts may be explained assuming that C atoms trap self-interstitial Si atoms (Si_i) during the ion implantation and the subsequent annealing process.^{2,3}

In the present study, we have investigated the as-implanted damage profiles produced by $^{11}\text{B}^+$ and $^{12}\text{C}^+$ implantations in *n*-type (100) oriented silicon wafers with resistivity of 4–11 $\Omega \text{ cm}$. All the implantations were

performed at an energy of 50 keV, at a dose rate of $0.4 \mu\text{A}/\text{cm}^2$ with $^{11}\text{B}^+$ to the doses of 1 and $4 \times 10^{15} \text{ cm}^{-2}$ or $^{12}\text{C}^+$ to doses ranging from 2×10^{14} to $5 \times 10^{15} \text{ cm}^{-2}$. The substrates were tilted by 7° with respect to the beam incidence direction to minimize the ion channeling. The defect profiles were analyzed by Rutherford backscattering spectrometry (RBS) with a 760 keV He^{++} beam aligned with the $\langle 100 \rangle$ crystal direction. The overall energy resolution of the RBS analysis was of 14 keV. The as-implanted damage was obtained using an iterative procedure to calculate the dechanneling background.⁹ In order to minimize room-temperature annealing effects, all the implanted samples were stored in liquid-nitrogen while waiting for the RBS analysis.

Figure 1 presents the damage depth profiles in samples implanted with $^{11}\text{B}^+$ or $^{12}\text{C}^+$ to the doses of $1 \times 10^{15} \text{ cm}^{-2}$ [Fig. 1(a)] and $4 \times 10^{15} \text{ cm}^{-2}$ [Fig. 1(b)]. For the lower dose, the damage profile due to the $^{11}\text{B}^+$ and $^{12}\text{C}^+$ implantations are almost similar, with concentration levels at the profile

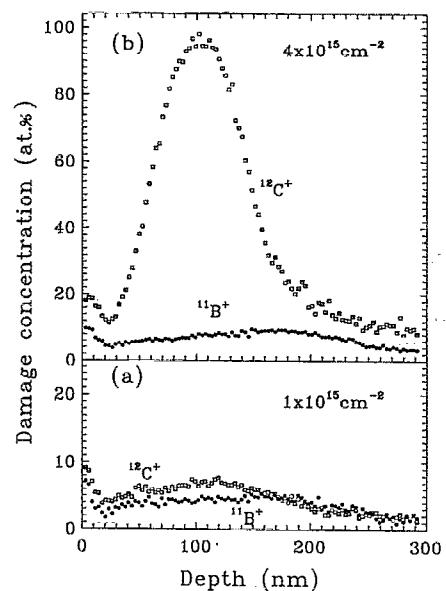


FIG. 1. Depth profiles of the damage created by $^{11}\text{B}^+$ and $^{12}\text{C}^+$ implanted Si at RT with energy of 50 keV and doses of $1 \times 10^{15} \text{ cm}^{-2}$ (a) and $4 \times 10^{15} \text{ cm}^{-2}$ (b).

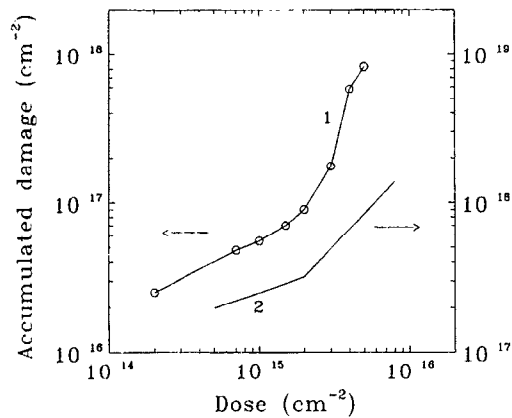


FIG. 2. Accumulated damage as function of the implanted $^{12}\text{C}^+$ dose at 50 keV (curve 1) and at 200 keV (Eisen and Welch) (curve 2).

peak of 5% and 7%, respectively. The increasing of the $^{11}\text{B}^+$ dose by a factor of 4 resulted in an increase of a factor of 2 in the accumulated damage. However, for the case of $^{12}\text{C}^+$ the same increasing of the dose led to a fourteen times increase of the damage concentration level at the profile peak.

The accumulated damage by $^{12}\text{C}^+$ implantation at 50 keV was studied for doses ranging from 2×10^{14} to $5 \times 10^{15} \text{ cm}^{-2}$. The accumulated damage is considered here as the depth integral of the damage concentration profile. Figure 2 compares the accumulated damage versus the implanted $^{12}\text{C}^+$ dose from the present work with those extracted from the article by Eisen and Welch,¹⁰ regarding a 200 keV $^{12}\text{C}^+$ implanted at a dose rate of $0.6 \mu\text{A}/\text{cm}^2$.

It is interesting to note that for doses $< 2 \times 10^{15} \text{ cm}^{-2}$ independently of the energy the accumulated damage increases with the square root of the dose (Φ). For the dose range $> 2 \times 10^{15} \text{ cm}^{-2}$, while the data of Eisen and Welch¹⁰ indicate that the accumulated damage depends linearly with Φ , our data vary with Φ^n ($2 < n < 3$).

The enhanced damage accumulation for $^{12}\text{C}^+$ doses above $2 \times 10^{15} \text{ cm}^{-2}$ can be explained considering that the dynamic annealing becomes strongly reduced when C concentration in the Si sample exceeds the $\approx 2 \times 10^{20} \text{ cm}^{-3}$ (the concentration at the profile peak for a $^{12}\text{C}^+$ implantation at 50 keV and dose of $3 \times 10^{15} \text{ cm}^{-2}$). Such enhancement of damage accumulation was not observed by Eisen and Welch,¹⁰ probably because for their implanted doses at energy of 200 keV the C concentrations are below $2 \times 10^{20} \text{ cm}^{-3}$.

The above results may be explained assuming that C atoms capture Si_i atoms produced in the collision cascades. The accumulation of trapped Si_i atoms in the neighborhood of the C atoms would form complex defect precipitates within the Si matrix. By increasing the C^+ dose, either the concentration of precipitates or their sizes should increase. Hence, enhancement of damage accumulation and reduction of the dynamic annealing take place.

Further evidence that the presence of a high C concentration influences the dynamic annealing in Si is shown in

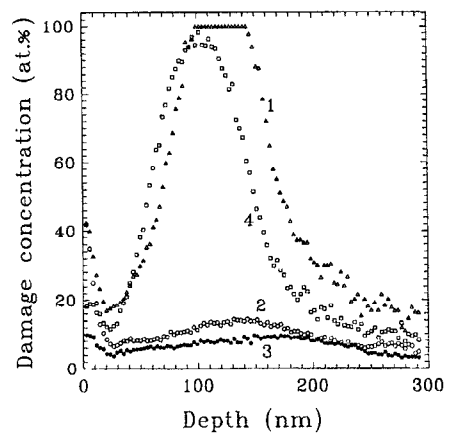


FIG. 3. Damage concentration depth profiles in Si samples implanted to doses of $4 \times 10^{15} \text{ cm}^{-2}$ and energy of 50 keV of $^{12}\text{C}^+$ at 100 °C followed by $^{11}\text{B}^+$ at RT (curve 1); $^{12}\text{C}^+$ at 100 °C (curve 2), $^{11}\text{B}^+$ at RT (curve 3) and $^{12}\text{C}^+$ at RT (curve 4).

Fig. 3, for the case of samples implanted first with $^{12}\text{C}^+$ (at 100 °C) and subsequently with $^{11}\text{B}^+$ (at RT) to equal doses of $4 \times 10^{15} \text{ cm}^{-2}$ (curve 1). The damage profile of as-implanted $^{12}\text{C}^+$ (curve 2) reveals that the accumulated damage during this hot implant is below the 15% level. During the subsequent $^{11}\text{B}^+$ implantation accumulated damage formed a buried amorphous layer with thickness of 50 nm, centered at the depth of 125 nm. For comparison the damage profiles due to a single RT implantation at a dose of $4 \times 10^{15} \text{ cm}^{-2}$ with $^{11}\text{B}^+$ (curve 3) and $^{12}\text{C}^+$ (curve 4) were included.

In summary, we have demonstrated that the dynamic annealing during the implantation of light ions, like $^{12}\text{C}^+$ or $^{11}\text{B}^+$, is noticeably reduced when the Si contains C in concentration $> 2 \times 10^{20} \text{ cm}^{-3}$. It is suggested that the implanted C atoms create trapping centers for Si_i atoms, generated in the collision cascades. The precipitation of Si_i at the trapping centers forms complex defect structures which are stable at room temperature.

This work was partially supported by Financiadora de Estudos e Projetos (Finep), Conselho Nacional de Pesquisas (CNPq) and Fundação de Amparo à Pesquisa do Estado do Rio Grande do Sul (FAPERGS).

¹J. Wang and M. Kulkarni, presented at the ECS Meeting, Extended Abstracts, No. 532, Florida (1980).

²H. Wong, N. W. Cheung, P. K. Chu, J. Liu, and J. W. Mayer, Appl. Phys. Lett. **52**, 1023 (1988).

³M. Tamura, T. Ando, and K. Ohyu, Nucl. Instrum. Methods B **59/60**, 572 (1991).

⁴H. Wong, N. W. Cheung, K. M. Yu, P. K. Chu, and J. Liu, Mater. Res. Soc. Symp. Proc. **147**, 97 (1989).

⁵S. Nishikawa and T. Yamaji, Appl. Phys. Lett. **62**, 303 (1993).

⁶S. Nishikawa, A. Tanaka, and T. Yamaji, Appl. Phys. Lett. **60**, 2270 (1992).

⁷J. R. Liefting, J. S. Custer, and F. W. Saris, Mater. Res. Soc. Symp. Proc. **235**, 179 (1992).

⁸J. P. de Souza and H. Boudinov, J. Appl. Phys. **74**, 6599 (1993).

⁹F. H. Eisen, in *Channeling*, edited by D. V. Morgan (Wiley, New York, 1973), p. 417.

¹⁰F. H. Eisen and B. Welch, in *European Conference on Ion Implantation* (Reading, UK, 1970), p. 227.